Diverse Roles of Glycine Residues Conserved in Photoactive Yellow Proteins

Yasushi Imamoto,*† Sanae Tatsumi,† Miki Harigai,†‡ Yoichi Yamazaki,† Hironari Kamikubo,† and Mikio Kataoka†

*Department of Biophysics, Graduate School of Science, Kyoto University, Kyoto 606-8502, Japan; †Graduate School of Materials Science, Nara Institute of Science and Technology, Ikoma, Nara 630-0192, Japan; and ‡Department of Cellular and Molecular Biology, Primate Research Institute, Kyoto University, Inuyama, Aichi 484-8506, Japan

ABSTRACT The role of glycine residues was studied by alanine-scanning mutagenesis using photoactive yellow protein, a structural prototype of PER ARNT SIM domain proteins, as a template. Mutation of glycine located close to the end of β-strands with dihedral angles disallowed for alanine (Gly-37, Gly-59, Gly-86, and Gly-115) induces destabilization of the protein structure. On the other hand, substitution for Gly-77 and Gly-82, incorporated into the fifth α-helix, slows the photocycle by 15–20 times, suggesting that these residues regulate the light-induced structural switch between dark-state structure and signaling-state structure. Most importantly, a significant amount of G29A is in the bleached state and showed a 1000-fold slower photocycle. As $O_{\varepsilon 2}$ of the carboxylic acid of Glu-46 is close enough for contact with C_α of Gly-29, alanine mutation perturbs this packing. Fourier transform infrared spectroscopy demonstrated that the $C{=}O_{\varepsilon 2}$ stretching mode of Glu-46 is 6 cm^{-1} upshifted in G29A, suggesting that C_α of Gly-29 acts as a proton donor for the C_α-H$\cdots O_{\varepsilon 2}$ hydrogen bond with Glu-46, which stabilizes the dark-state structure. During the photocycle, Glu-46 becomes negatively charged by donating a proton to the chromophore, resulting in breakage of this hydrophobic packing and consequent conformational change of the protein.

INTRODUCTION

Of 20 amino acids in proteins, glycine is peculiar in that it has no side chains. Low levels of internal steric hindrance allow dihedral angles (ϕ, ψ angles) rare for other amino acid residues (disallowed region of Ramachandran plot). Glycine can form a sharp loop-like β-turn connecting secondary structure elements. Thus flexibility of glycine is essential for the overall fold of most proteins. Absence of a side chain provides the spatial tolerance as well. For example, collagen has glycine at every third position. Due to the absence of side chains in glycine, three helical chains can be packed tightly together to form the collagen superhelix. Therefore, glycine is likely to have a unique role, given its flexible dihedral angle and/or small dimensions. Replacement of most glycine residues would cause a marked effect. This is informative for understanding the mechanism of protein folding and conformational changes. In this work, glycine residues of photoactive yellow protein (PYP) and their role were systematically examined by substitution with alanine.

PYP is a water-soluble photoreceptor protein composed of 125 amino acid residues and a *p*-coumaric acid chromophore binding to a cysteine residue by a thioester bond (1–3). Due to its simple structure, as well as the availability of the tertiary structure at the atomic level (4,5), it is a good target for investigating the photoreaction and subsequent conformational changes based on protein structure. PYP was first found in the purple photosynthetic sulfur bacterium, *Halorhodospira halophila* (6,7). The primary structures of four PYPs from *Rhodothalassium salexigens* (8,9), *Halochromatium salexigens* (9), *Rhodobacter sphaeroides* (10), and *Rhodobacter capsulatus* (11) are also available. These PYPs are highly homologous, with 44 out of 125 amino acid residues perfectly conserved between them. Although PYPs from *Hr. halophila*, *Rt. salexigens*, and *Hc. salexigens* have a single absorption band in the visible region, PYPs from *Rb. sphaeroides* and *Rb. capsulatus* are mixtures of yellow and bleached states (12). Amino acid sequences of the PYP domains of Ppr (PYP-phytochrome related histidine kinase) from *Rhodocista centenum* (13) and Ppd (PYP/bacteriophytochrome/diguanylate cyclase/phosphodiesterase) from *Thermochromatium tepidum* (12) are available. The former is yellow colored like *Hr. halophila* PYP, whereas the latter is bleached under physiological conditions due to the lack of a glutamic acid at position 46, which is important for deprotonation of the phenolic oxygen of the chromophore. Consequently, 23 amino acid residues are perfectly conserved between seven PYP-like proteins and domains.

A schematic drawing of the secondary structure of *Hr. halophila* PYP is shown in Fig. 1. *Hr. halophila* PYP has 13 glycine residues (1,14,15). Gly-29, Gly-37, Gly-59, Gly-77, and Gly-86 are perfectly conserved between seven PYPs (Fig. 1, Table 1). Gly-7 is conserved, except for the PYP domain from *Tc. tepidum*, and Gly-47, Gly-51, Gly-82, and Gly-115 are conserved between four or five PYPs. In contrast, Gly-21, Gly-25, and Gly-35 are less conserved.

Gly-7, Gly-37, Gly-51, Gly-59, Gly-86, and Gly-115, indicated by hexagonal stars in Fig. 1 *a*, have dihedral angles

Submitted October 9, 2007, and accepted for publication December 21, 2007.

Address reprint requests to Yasushi Imamoto, Dept. of Biophysics, Graduate School of Science, Kyoto University, Kyoto 606-8502, Japan. Tel.: 81-75-753-4243; Fax: 81-75-753-4210; E-mail: imamoto@vision-kyoto-u.jp.

Editor: Janos K. Lanyi.

0006-3495/08/05/3620/09 $2.00

doi: 10.1529/biophysj.107.123414

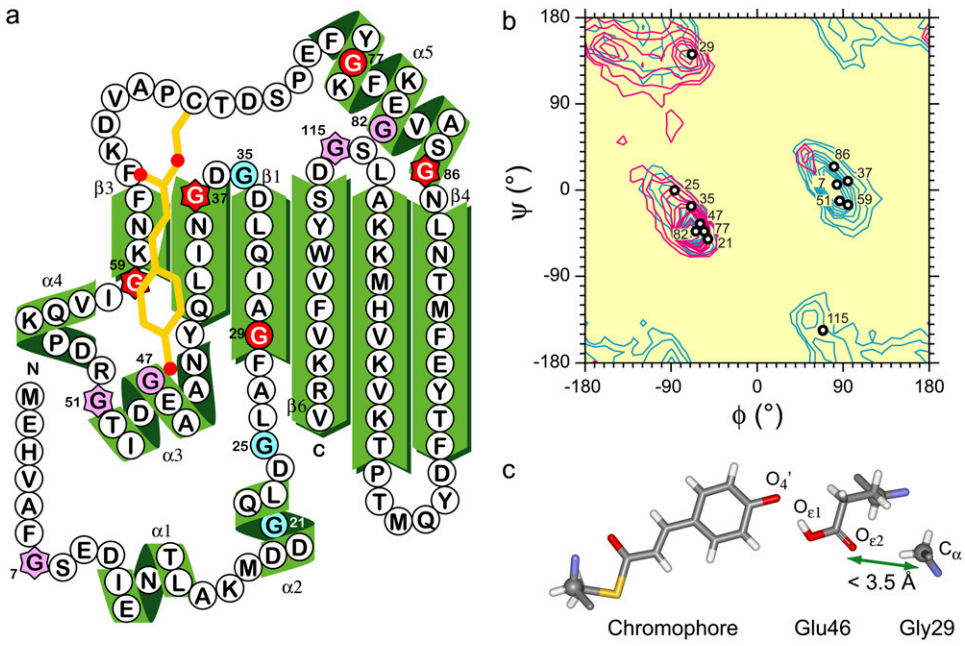

FIGURE 1 (*a*) Schematic drawing of the secondary structure of *Hr. halophila* PYP. Glycine residues are colored. Conserved and partially conserved glycine residues are shown in red and pink, respectively, and cyan shows nonconserved glycine residues. Glycine residues that have disallowed ϕ, ψ angles are indicated by a hexagonal star. (*b*) A Ramachandran plot of glycine residues (1NWZ). Contours indicated in cyan and magenta show the favored ϕ, ψ angles for glycine and alanine, respectively (16). (*c*) Spatial relationship of Gly-29, Glu-46, and the chromophore.

disallowing alanine (16) (Fig. 1 *b*, Table 2). Except for Gly-7, they are located at the end of an α-helix or β-strand. Therefore, substitutions at these positions might perturb the protein backbone. In addition, some glycine residues are close to the chromophore binding pocket (Gly-47, Gly-51, and Gly-29). These findings suggest that glycine residues may be the key residues determining the structure and function of PYP.

The role of glycine in PYP has been extensively investigated for a PER ARNT SIM (PAS) core segment at positions 47 and 51 (17). Phenolic oxygen of PYP chromophore is hydrogen bonded with Glu-46 and Tyr-42, and this interaction is stabilized by Arg-52. The fact that the neighboring residues of Glu-46 and Arg-52 are glycines strongly suggests that the flexibility of glycine is essential for the function of Glu-46 and Arg-52. Crystallography of mutants in which these residues was replaced by Ser (G47S, G51S, and G47S/G51S) demonstrated no significant alteration of the protein structure, but recoveries of G47S and G51S from their M intermediates (also called I_2 or pB) are 3–4 times slower than wild-type (WT) (17). As these glycine residues are not perfectly conserved, more essential glycine might be present in conserved glycines.

In this study, the role of all glycine residues in *Hr. halophila* PYP were studied by characterizing mutants in which glycine was replaced by alanine by thermal denaturation, pH titration of the chromophore, and flash photolysis over a millisecond timescale. As G29A showed striking alterations of properties, it was further characterized using Fourier transform infrared (FTIR) spectroscopy.

MATERIALS AND METHODS

Sample preparation

PYP mutant genes were prepared according to a standard protocol (15,18). To substitute alanine for glycine, GGC, GGT, and GGG of the original gene were replaced by GCC, GCT, and GCG, respectively. Apoproteins of mutants were heterologously overexpressed by *Escherichia coli*, then reconstituted by adding *p*-coumaric anhydride in the presence of 4 M urea (3,15). Holoproteins of PYP mutants were purified by diethylaminoethyl-Sepharose column chromatography (Amersham Biosciences, Piscataway, NJ) (15,18) and suspended in 10 mM MOPS (3-(*N*-morpholino)propanesulfonic acid) buffer at pH 7.0. Ultraviolet (UV)-visible absorption spectra were recorded by a Shimadzu (Kyoto, Japan) UV-2400PC recording spectrophotometer. Purity of the sample was evaluated using an optical purity index (ratio of

TABLE 1 Conservation of glycine residues

	Position												
	7	21	25	29	35	37	47	51	59	77	82	86	115
Hr. halophila	G	G	G	G	G	G	G	G	G	G	G	G	G
Rt. salexigens	G	A	D	G	E	G	G	G	G	G	G	G	G
Hc. salexigens	G	Q	Q	G	A	G	E	G	G	G	G	G	D
Rb. sphaeroides	G	Q	Y	G	R	G	G	N	G	G	F	G	G
Rb. capsulatus	G	A	S	G	R	G	G	G	G	G	F	G	G
Rc. centenum	G	A	A	G	G	G	S	G	G	G	G	G	P
Tc. tepidum	I	D	R	G	A	G	V	N	G	G	G	G	P

TABLE 2 Properties of alanine mutants and role of glycine residues in PYP

Position	Dihedral angles	Conservation	Properties of Ala mutants				Role of glycine
			λ_{max} (nm)	$T_{1/2}$ (°C)*	$pK_a^{\dagger}$	k (s^{-1})	
–‡	–	–	446	90.3 ± 0.2	2.9	5.49 ± 0.02	
29	β-strand	Yes	442	99.6 ± 1.2	9.1	0.00476 ± 0.0005	H^+ donor for C_α-H···O hydrogen bond
77	α-helical	Yes	445	83.7 ± 0.1	2.8	0.290 ± 0.001	Facilitate the photocycle
82	α-helical	Partially	445	88.8 ± 0.4	3.5	0.366 ± 0.002	Facilitate the photocycle
47	α-helical	Partially	443	90.3 ± 0.1	2.7	2.93 ± 0.01	Form the chromophore binding site
51	Disallowed	Partially	447	89.6 ± 0.2	3.7	0.482 ± 0.003	Form the chromophore binding site
37	Disallowed	Yes	446	81.9 ± 0.1	3.0	2.64 ± 0.01	Stabilize the dark-state structure
59	Disallowed	Yes	446	82.8 ± 0.1	3.0	4.71 ± 0.02	Stabilize the dark-state structure
86	Disallowed	Yes	446	85.6 ± 0.1	2.9	4.57 ± 0.03	Stabilize the dark-state structure
115	Disallowed	Partially	445	86.0 ± 0.9	2.7	8.27 ± 0.04	Stabilize the dark-state structure
7	Disallowed	Partially	446	91.6 ± 0.3	2.9	1.74 ± 0.01	No important role
21	α-helical	No	446	89.6 ± 0.1	2.4	6.37 ± 0.03	No important role
25	α-helical	No	446	90.2 ± 0.1	2.5	6.50 ± 0.04	No important role
35	α-helical	No	446	92.2 ± 0.1	2.7	5.47 ± 0.03	No important role

*Error is the standard deviation of fit coefficients estimated by the trace from a single experiment.
†Errors <0.1.
‡Values for WT.

absorbance at 277 nm to λ_{max}). For WT and mutants except G29A, the optical purity index was 0.43–0.46 (pH 7.0). For G29A an optical purity index was estimated at pH 2.0, where G29A is fully in the bleached form (λ_{max} = 350 nm). The ratio of absorbance at 277 nm to 350 nm was 0.84. These results demonstrate that the purity of these samples is >95%.

Thermal denaturation

Thermal denaturation experiments were performed on a JASCO (Tokyo, Japan) J-725 circular dichroism (CD) spectropolarimeter, as reported previously (19). The negative CD signal at 222 nm linearly decreased with temperature before denaturation. This change was empirically approximated by a linear line, subtracted from experimental data as a baseline. Using ellipticity of the native and denatured states at 222 nm, the fraction of native state (f) at each temperature was calculated. f was fitted to the following equation:

$$f = \frac{1}{1 + \exp\left(\frac{\Delta H}{R}\left(\frac{\Delta S}{\Delta H} - \frac{1}{T}\right)\right)}, \quad (1)$$

where ΔH and ΔS are enthalpy and entropy of denaturation, R is the gas constant, and T is temperature. $\Delta H/\Delta S$ shows the midpoint temperature ($T_{1/2}$), used as a measure of thermal stability.

pH titration of the chromophore

The phenolic oxygen of the chromophore was titrated by adding HCl or NaOH. WT and mutants, except G29A, showed simple conversion from the yellow form to the colorless form after acidification. Absorbance at λ nm (Abs_λ) against pH was fitted to the following equation:

$$Abs_\lambda = \frac{\varepsilon_C + \varepsilon_Y \times 10^{n(pH-pK)}}{1 + 10^{n(pH-pK)}} \times c, \quad (2)$$

where ε_Y and ε_C are the molar extinction coefficients at λ nm for the yellow and colorless forms, respectively, c is total molar concentration, and n is a cooperativity constant. As pH-dependent absorbance change of G29A showed four plateaus or inflection points, equilibrium containing yellow form ($G29A^Y$), colorless form ($G29A^C$), and two putative intermediate states ($G29A^{IS1}$ and $G29A^{IS2}$) was assumed as follows:

$$G29A^Y \underset{-n_1H^+}{\overset{+n_1H^+}{\rightleftharpoons}} G29A^{IS1} \underset{-n_2H^+}{\overset{+n_2H^+}{\rightleftharpoons}} G29A^{IS2} \underset{-n_3H^+}{\overset{+n_3H^+}{\rightleftharpoons}} G29A^C. \quad (3)$$

In this equilibrium, the concentration of each component is expressed as follows:

$$[G29A^Y] = \frac{c}{1 + 10^{-n_1(pH-pK_1)} + 10^{-n_1(pH-pK_1)-n_2(pH-pK_2)} + 10^{-n_1(pH-pK_1)-n_2(pH-pK_2)-n_3(pH-pK_3)}} \quad (4)$$

$$[G29A^{IS1}] = \frac{c}{1 + 10^{n_1(pH-pK_1)} + 10^{-n_2(pH-pK_2)} + 10^{-n_2(pH-pK_2)-n_3(pH-pK_3)}} \quad (5)$$

$$[G29A^{IS2}] = \frac{c}{1 + 10^{n_1(pH-pK_1)+n_2(pH-pK_2)} + 10^{+n_2(pH-pK_2)} + 10^{-n_3(pH-pK_3)}} \quad (6)$$

$$[G29A^C] = \frac{c}{1 + 10^{n_1(pH-pK_1)+n_2(pH-pK_2)+n_3(pH-pK_3)} + 10^{+n_2(pH-pK_2)+n_3(pH-pK_3)} + 10^{n_3(pH-pK_3)}}, \quad (7)$$

where c is total molar concentration, and K_1, K_2, and K_3 are equilibration constants for their respective equilibria. Absorbance at λ nm (Abs_λ) for G29A was thus fitted using the following equation.

$$Abs_\lambda = \varepsilon_Y[\mathrm{G29A^Y}] + \varepsilon_{IS1}[\mathrm{G29A^{IS1}}] + \varepsilon_{IS2}[\mathrm{G29A^{IS2}}] + \varepsilon_C[\mathrm{G29A^C}], \quad (8)$$

where ε_Y, ε_{IS1}, ε_{IS2}, and ε_C are the molar extinction coefficients at λ nm for $\mathrm{G29A^Y}$, $\mathrm{G29A^{IS1}}$, $\mathrm{G29A^{IS2}}$, and $\mathrm{G29A^C}$, respectively.

Flash photolysis

Transient spectra after photoexcitation of PYP mutants were measured using a multichannel charge-coupled device (CCD)/fiber optic spectroscopy system (S2000 system; Ocean Optics, Dunedin, FL) (20). An excitation pulse (>410 nm, duration = 150–180 μs) was generated by a short arc xenon flash lamp (SA200E; Eagle, Kawasaki, Japan), then passed through a glass cut-off filter (Y43; Asahi Techno Glass, Chiba, Japan). Each flash converted 10%–20% of pigments to M intermediates, from which excitation energy was calculated to be within the linear range reported previously (21).

FTIR spectroscopy

FTIR spectra were recorded with a BioRad FTS-6000 FTIR spectrophotometer equipped with an Oxford (Witney, Oxfordshire, UK) Optistat DN optical cryostat (22). PYP or mutant was dissolved in the buffer (100 mM TAPS (3-{[2-hydroxy-1,1-bis(hydroxymethyl)ethyl]amino}propane-1-sulfonic acid), 200 mM NaCl, pH 8.0) at high concentration (~100 mg/ml) and placed between two CaF_2 windows with a 7 μm spacer. Difference FTIR spectra were calculated by subtracting dark state spectra from photo steady state spectra generated by a blue light at 436 nm passed through an optical interference filter (43161, Edmund Optics, Barrington, NJ).

RESULTS

Absorption spectra and far-UV CD spectra of PYP mutants

Apoprotein from a site-directed mutant was expressed by *E. coli* then reconstituted into holoprotein by adding *p*-coumaric anhydride. UV-visible absorption spectra measured at pH 7.0 are shown in Fig. 2 *a*. WT shows a single bell-shaped absorption spectrum, with maximum at 446 nm in the visible region. The absorption maximum of G47A was located at 443 nm and the absorption maximum of G51A was located at 447 nm (Table 2). G29A was in the equilibrium between the yellow (442 nm) and colorless (360 nm) forms, with the latter dominant at neutral pH. Other mutants had absorption spectra comparable to WT. Secondary structures of these mutants were studied by far-UV CD spectra (Fig. 2 *b*). Results demonstrated that the negative CD signal of G37A at 210 nm was larger than WT, suggesting that some portion of the secondary structure is unfolded. The negative CD peak of G29A was 2-nm blue shifted. The maximal difference between CD spectra of G29A and WT was located at ~222 nm, suggesting that the α-helix would be partially unfolded in G29A. CD spectra for the other mutants are comparable to WT, indicating that the replacement of glycine residues, except at positions 29 and 37, does not affect the secondary structure of PYP.

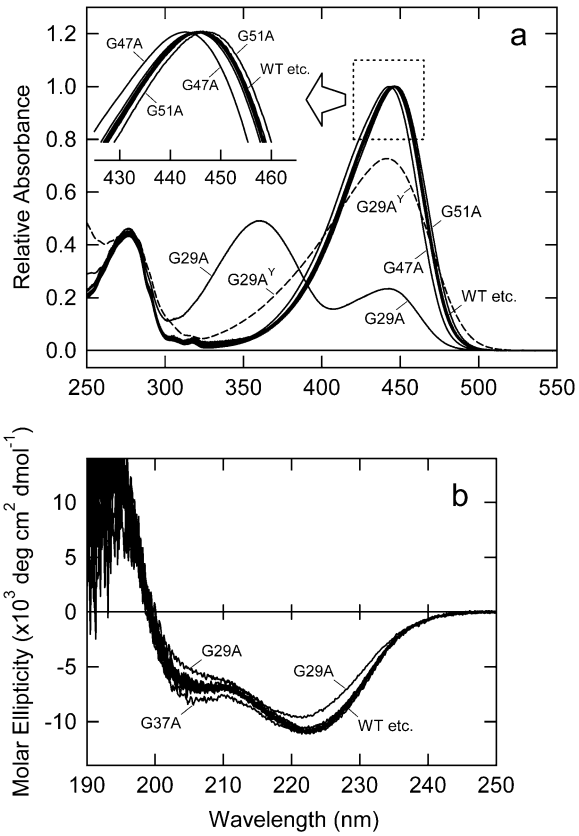

FIGURE 2 UV-visible absorption spectra and far-UV CD spectra of PYP mutants. (*a*) Absorption spectra of WT, G7A, G21A, G25A, G29A, G35A, G37A, G47A, G51A, G59A, G77A, G82A, G86A, and G115A were measured at pH 7.0, 20°C. The major part of G29A is in a colorless form ($\mathrm{G29A^C}$; absorption maximum, 360 nm) in this condition. The absorption spectrum of the yellow form of G29A ($\mathrm{G29A^Y}$) was calculated (see text) and is shown as a broken line. Although absorption maxima of G47A and G51A were 3 nm blue shifted and 1 nm red shifted, respectively, maxima for other mutants agreed with WT. (*b*) CD spectra were measured under the same conditions. CD spectra of mutants other than G29A and G37A agreed with WT.

Thermal denaturation experiments

Thermal stability of mutants was studied by denaturation experiments using far-UV CD. The temperature of the sample was raised 1°C/min, and ellipticity at 222 nm was recorded at each temperature. If PYP is folded, a negative CD signal due to the α-helix and β-sheet is observed (Fig. 2 *b*) while intensity is lowered for the denatured state (23). Midpoint temperature ($T_{1/2}$) estimated by Eq. 1 was used as the measure of stability (Table 2). The negative CD signal of G115A was decreased by warming to 87°C but increased after further warming (data not shown), probably due to the formation of an amyloid-like structure (24). Therefore, to estimate $T_{1/2}$, ellipticity for the denatured state of G115A was assumed to be the same as WT. $T_{1/2}$ of G37A, G59A, G77A, G86A, and G115A were 4°C–8°C lower than WT (Table 2), indicating that replacement of glycine residues at these positions significantly destabilizes the PYP structure. It is important to note that the dihedral angles of Gly-37, Gly-59, Gly-86, and Gly-115 are unfavorable for alanine (Fig. 1). Unexpectedly, $T_{1/2}$ of G29A was significantly higher than

WT. However, this finding is likely to be an artifact as α-helices, less stable than a β-sheet in the PYP structure, are partially unfolded in G29A (Fig. 2 *b*).

pH titration of the chromophore

Upon acidification, PYP is bleached by protonation of the chromophore (6,18,25). pH titration of mutants except G29A showed pH-dependent equilibria between the yellow and colorless forms like WT (data not shown). pK_a values estimated by fitting the absorbance change to Eq. 2 are summarized in Table 2. pK_a values for G51A and G82A were larger than WT (3.7 and 3.5, respectively), whereas the others were comparable or lower.

pH titration of G29A was complicated (Fig. 3 *a*). The yellow form is dominant only at pH > 9 but denatured at pH 11.6, as shown by the absorption maximum at 400 nm (26,27). Over a wide pH range (pH 4–8), G29A had its main absorption band at 360 nm and spectral shoulder at 440 nm. This resembles findings for Y42A (18). Typical absorbance changes at 490, 441, and 370 nm were plotted against pH (Fig. 3 *b*). As there were two inflection points in addition to two plateaus for the acidic (pH 2) and alkaline (pH 10) forms, equilibrium between four states, yellow form ($G29A^Y$), colorless form ($G29A^C$), and two putative intermediate states ($G29A^{IS1}$ and $G29A^{IS2}$), was assumed. Absorbance changes

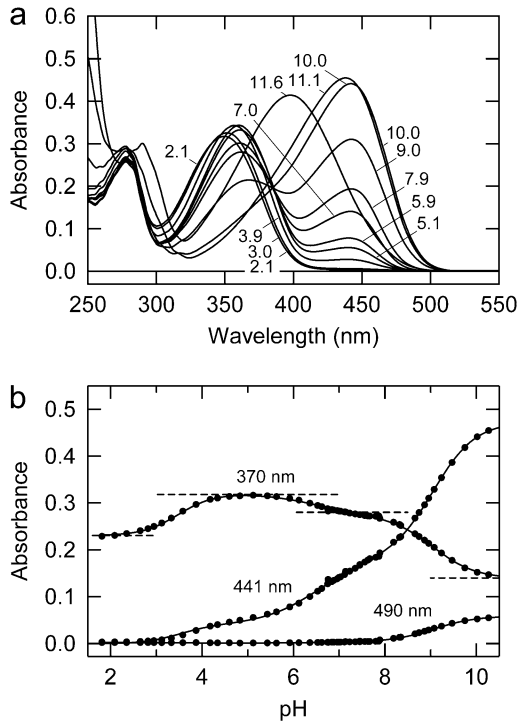

FIGURE 3 pH titration of G29A. (*a*) Absorption spectra of G29A at various pH. pH values are indicated in the figure. (*b*) Absorbance at 490, 441, and 370 nm is plotted against pH and fitted using Eq. 8. pK_1, pK_2, and pK_3 were estimated to be 9.07, 6.53, and 3.49, and n_1, n_2, and n_3 were estimated to be 0.94, 0.71, and 1.12, respectively.

at 490, 441, and 370 nm were simultaneously fitted by Eq. 8 using a global fitting program, producing values of 9.07 for pK_1, 6.53 for pK_2, and 3.49 for pK_3. Cooperativity constants of n_1, n_2, and n_3 were estimated to be 0.94, 0.71, and 1.12, respectively. Using these values and the measured spectra, the absorption spectrum of $G29A^Y$ was calculated (Fig. 2 *a*).

The absorption spectrum of $G29A^Y$ is broadened on the short wavelength side, suggesting the possible presence of 360-nm species. The $G29A^Y$ spectrum was reproduced by the sum of three Gaussian curves at 455 nm (amplitude = 0.38, width = 54 nm), 429 nm (amplitude = 0.38, width = 68 nm), and 393 nm (amplitude = 0.24, width = 99 nm), compared to 454 nm (amplitude = 0.55, width = 40 nm), 433 nm (amplitude = 0.54, width = 56 nm), and 408 nm (amplitude = 0.23, width = 80 nm) for the WT spectrum (not shown). Therefore, the broad spectrum of $G29A^Y$ is accounted for by a 15-nm blue shift and the broadening of the third component rather than the presence of 360-nm species.

Flash photolysis over a millisecond timescale

On photon absorption, PYP is transiently bleached in ~1 ms, then recolored in ~500 ms (28). PYP mutants were excited by a yellow flash (>410 nm), then subsequent spectral changes in the 100 ms timescale were recorded using a CCD multichannel spectrophotometer (Fig. 4). In the time resolution here (~20 ms), an absorbance decrease at 446 nm and an absorbance increase at 350 nm were observed just after excitation (Fig. 4 *a*), showing conversion from dark state to M intermediate (= pB or I_2). Subsequently, absorbance at 446 and 350 nm reverted to the dark state. Absorbance changes for recovery were plotted against time after excitation in a logarithmic timescale (Fig. 4 *b*). Traces were fitted by single-exponential curves, and rate constants were estimated (Table 2). Rate constants of mutants varied by more than three orders of magnitude. Decay of $G29A_M$ was 1000-fold slower than WT, possibly due to denaturation of $G29A_M$ like its dark state. $G51A_M$, $G77A_M$, and $G82A_M$ showed a 10–20-fold slower decay than WT_M, suggesting that these glycine residues are involved in the light-induced conformational change.

The positive band in the difference spectra for formation of M intermediate was blue shifted for G77A and G82A, whereas bands from other mutants agreed with WT (Fig. 4 *a*, *inset*). This demonstrates the shift of equilibrium between PYP_M^{acid} (I_2 or pB′) and PYP_M^{alkali} ($I_{2'}$ or pB) (29) toward the latter in G77A and G82A.

FTIR spectroscopy of G29A

Mutation of Gly-29 yielded the most significant alteration among the 13 glycine residues of *Hr. halophila* PYP. As Gly-29 is located at the hinge position of the N-terminal cap and PAS core (30), it was first assumed that the strain of these segments resulting from alanine substitution may cause

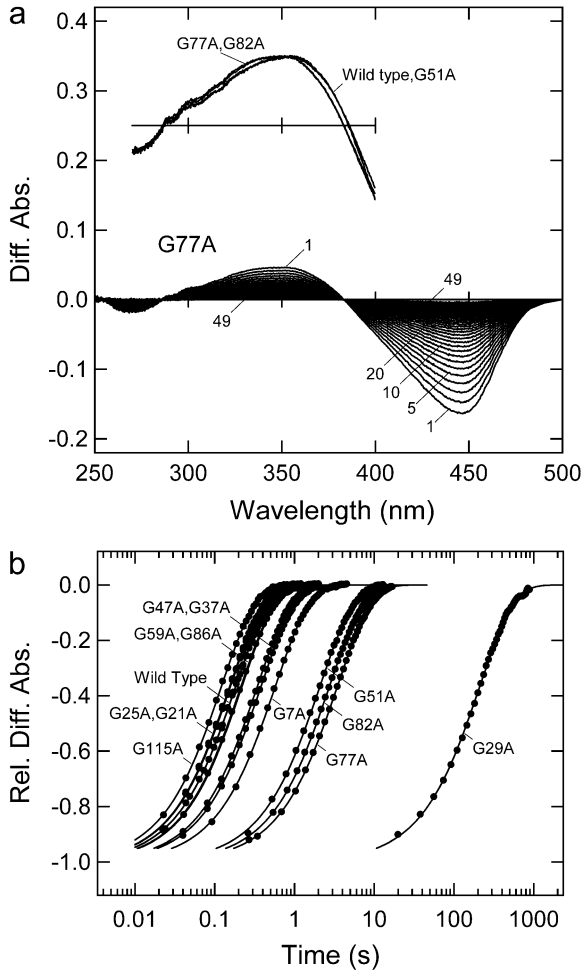

FIGURE 4 Thermal recovery of dark states from M intermediates. (*a*) G77A (pH 7.0) was excited by a yellow flash (>410 nm), then subsequent spectral changes were recorded every 340 ms. Inset: transient difference spectra for WT, G51A, G77A, and G82A are compared. (*b*) Absorbance changes at difference maxima (440–450 nm) after flash excitation were plotted against time after excitation. Data were fitted by the single-exponential curves.

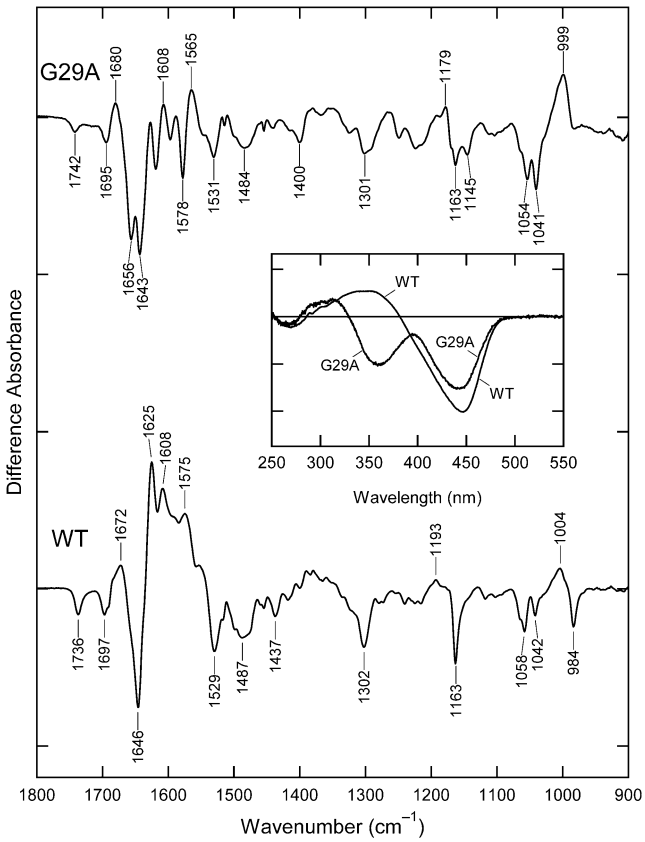

FIGURE 5 Difference FTIR spectra between dark state (negative) and photo steady state (positive). Photo steady state was generated by illuminating with 436 nm light at 4°C. (*Inset*) UV-visible difference spectra measured under the same conditions.

partial bleaching of PYP. Therefore, the N-terminal cap of G29A was cleaved by chymotrypsin to release this strain. Although truncation of the N-terminal cap does not bleach PYP (31,32), the yellow color was not recovered (data not shown). As the dihedral angle of Gly-29 is located in a β-strand region (Fig. 1 *b*), flexibility of Gly-29 is unlikely to be important for PYP. The crystal structure of dark-state PYP demonstrates that H_α of Gly-29 is in van der Waals contact with $O_{\varepsilon 2}$ of Glu-46 (Fig. 1 *c*), suggesting an interaction between Gly-29 and Glu-46. Therefore the interaction involving Gly-29 was characterized using FTIR spectroscopy.

UV-visible difference spectra between the dark and photo steady states generated by 436-nm light are shown in the inset of Fig. 5. WT showed a broad negative band at 446 nm and a positive band at 350 nm, indicating bleaching of the dark state and formation of PYP_M, respectively. G29A showed two negative bands at 442 and 370 nm while illuminated with 436-nm light to not excite $G29A^C$. This indicates that $G29A^Y$ and $G29A^C$ are in equilibrium and a rapid repopulation takes place after the loss of $G29A^Y$ from light exposure. In this condition, difference FTIR spectra between dark and photo steady states were recorded for WT and G29A (Fig. 5). The intense negative band of WT at 1163 cm^{-1} is characteristic of the deprotonated *trans* chromophore (33,34). The 1163 cm^{-1} band was reduced; however, a band at 1145 cm^{-1} and a shoulder at ~1170 cm^{-1} appeared in the G29A spectrum. As they are also observed for the acidic (bleached) forms of WT and mutants (35), this mode is characteristic of the protonated *trans* chromophore. As the absorbance decrease attributable to $G29A^Y$ and $G29A^C$ in the infrared (1163 and 1145 cm^{-1}, respectively) and UV-visible regions (442 and 370 nm, respectively) were comparable, the negative region of the FTIR spectrum of G29A represents an approximate 1:1 mixture of $G29A^Y$ and $G29A^C$.

The $C{=}O_{\varepsilon 2}$ stretching mode of the carboxylic acid of Glu-46 (protonated) is observed at 1736 cm^{-1} for WT in the dark state (34). A corresponding band of G29A was present at 1742 cm^{-1}. Intensity of this band was significantly reduced, whereas the bandwidth was comparable to WT, suggesting

that G29A in the dark state in part has this mode. Negative bands in the G29A spectrum are attributable to a mixture of $G29A^Y$ and $G29A^C$. For WT, Glu-46 is protonated in the dark state (yellow form) but deprotonated in PYP_M (bleached form). Therefore, it is reasonable to attribute the 1742 cm^{-1} band to $G29A^Y$, that is, Glu-46 of $G29A^Y$ is protonated in the dark state like WT, whereas Glu-46 of $G29A^C$ is deprotonated. Absence of the complementary positive band shows that Glu-46 of $G29A_M$ is deprotonated. The $C{=}O_{\varepsilon 2}$ stretching mode of $G29A^Y$ was 6-cm^{-1} upshifted from WT, showing that the hydrogen bond involving Glu-46 is weakened in $G29A^Y$.

DISCUSSION

In this study, 13 glycine residues of *Hr. halophila* PYP were replaced by alanine, and the mutants were characterized. Substitution for conservative glycine residues caused significant changes in properties, and detailed inspection based on the tertiary structure shows that the glycine residues of PYP perform various roles (Table 2).

Replacement of Gly-29 showed the most striking effect on properties of PYP of all the glycine residues. G29A is in the equilibrium between yellow form ($G29A^Y$) and colorless form ($G29A^C$) at neutral pH and shows an extremely slow photocycle. $G29A^Y$ was enriched by cooling and addition of NaCl and ammonium sulfate (data not shown), suggesting that $G29A^C$ assumes a less packed structure than does $G29A^Y$ (36). H_α of Gly-29 is in van der Waals contact with $O_{\varepsilon 2}$ of Glu-46 (Fig. 1 *c*). Previous crystallography has demonstrated that the distance from $O_{\varepsilon 2}$ of Glu-46 to C_α of Gly-29 is 3.32 (Protein Data Bank (PDB) 2PHY) (4), 3.34 (PDB 2D01) (37), 3.40 (PDB 1NWZ) (5), or 3.45 Å (PDB 1OTB) (38). This proximity is also seen in Ppr (PDB 1MZU, 3.36–3.49 Å for chains A–C) (39), suggesting that it is a common arrangement in PYPs. The phenolic oxygen of the chromophore ($O_{4'}$) is located on the opposite side and hydrogen bonded with the $O_{\varepsilon 1}$-H of Glu-46. Replacement of Gly-29 by alanine substitutes a methyl group for H_α in proximity to Glu-46. The methyl group added to this position should not be accommodated without perturbation of the interaction between Glu-46 and the chromophore. Gly-29 thus provides space to accommodate the carboxylic acid of Glu-46.

FTIR spectroscopy demonstrated that the $C{=}O_{\varepsilon 2}$ stretching mode of Glu-46 is located at 1736 cm^{-1} in WT and shifts to 1742 cm^{-1} in G29A. The upshift of 6 cm^{-1} indicates that the mutation of Gly-29 to Ala significantly weakened the hydrogen bond(s) involving Glu-46. If the hydrogen bond between $O_{\varepsilon 1}$-H and $O_{4'}$ of the chromophore is weakened, the absorption spectrum of G29A should be red shifted (40). Therefore, these findings suggest that the additional hydrogen bond is present between $O_{\varepsilon 2}$ and C_α-H of Gly-29. It should be noted that this is a CH···O hydrogen bond, which is weaker than a conventional OH···O or NH···O hydrogen bond (41,42), thus the $C{=}O_{\varepsilon 2}$ stretching frequency of Glu-46 (1736 cm^{-1}) is higher than that of the carboxylic acid forming two hydrogen bonds (1703–1710 cm^{-1}) (43). Replacement of Gly-29 by Ala brings about the displacement of Glu-46 by steric hindrance, which would also cause the altered properties of G29A.

If Glu-46 is protonated, $\delta+$ of C_α of Gly-29 and $\delta-$ of $O_{\varepsilon 2}$ of Glu-46 are electrostatically balanced, and the packing of this part would be stabilized by hydrophobic interaction as well as a C_α-H···$O_{\varepsilon 2}$ hydrogen bond. In the PYP photocycle, a proton of $O_{\varepsilon 1}$ is transferred to $O_{4'}$ upon conversion from PYP_L (= I_1 or pR) to PYP_M (34,44,45). The negatively charged Glu-46 would abolish the hydrophobic effect, and then packing would not be further maintained solely by a weak C_α-H···$O_{\varepsilon 2}$ hydrogen bond. As the generation of negative charge at position 46 is essential for the protein conformational change of PYP (45,46), Glu-46 is proposed as an epicenter of the protein quake, although the function of the negative charge is unclear. The experiments here show that breakage of hydrophobic packing by the generation of negative charge would be the essence of the protein quake. The results of this study provide a clear example that the CH···O hydrogen bond, for which importance in protein appears to be in dispute, is present in the core portion for the structure and function of protein.

Substitutions of Gly-77 and Gly-82 by alanine shift pK_a of the chromophore or thermal stability in the dark state. It is more noticeable that $G77A_M$ and $G82A_M$ were markedly stabilized (~20 times), suggesting that Gly-77 and Gly-82 during the photocycle take more essential roles than in the dark state. The transient difference maxima of these mutants were slightly blue shifted from WT (Fig. 4 *a*), indicating that the equilibrium between PYP_M^{acid} and PYP_M^{alkali} (29) shifts toward the latter. Gly-77 and Gly-82 are located in α5-helix, which interacts with the β-scaffold segment (β4–β6). However, the side chain of position 77 directs outward from the protein, and the addition of a methyl group is unlikely to perturb the interaction with the β-sheet. Glycine destabilizes the α-helix (47), and thus the presence of two glycine residues suggests that the α5 of WT is less stable than G77A and G82A. NMR studies have shown that M intermediates formed from WT and Δ25 (PYP lacking N-terminal 25 amino acid residues) show an unfolding of the N-terminal half of α5 (48,49). Our previous CD experiment also demonstrated that the loss of CD is explained by a structural change of the long α-helix (α5 and/or α3) (22). These results suggest that Gly-77 and/or Gly-82 act as the hinge between the unfolded and native parts of α5. The shift of equilibrium between PYP_M^{acid} and PYP_M^{alkali} toward a more disordered state (PYP_M^{alkali}) in G77A and G82A suggests, however, that stable α5 is favorable for PYP_M^{alkali}. Thus the equilibrium between two M-intermediates would not depend solely on the stability of α5. The strain at position 77 and/or 82 would disorder the overall structure of M intermediate.

The slow recovery of $G77A_M$ and $G82A_M$ seems to suggest that the refolding of the partially unfolded structure of

M intermediate is suppressed by replacing Gly-77 or Gly-82 with alanine. However, as the *cis-trans* reisomerization of the chromophore is a rate-determining step of the recovery of the dark state (50,51), the slow recovery should be accounted for by the structure of the chromophore binding site of PYP_M rather than the rate of refolding. Therefore, the flexibility of Gly-77 and Gly-82 are necessary to form the chromophore binding site facilitating *cis-trans* isomerization.

Gly-51 neighbors Arg-52, which stabilizes the anionic form of the chromophore but is not involved in the color regulation (15). Thermal stability of G51A was almost the same as WT, but pK_a was 3.7 and the lifetime of $G51A_M$ was 11 times longer than PYP_M. These properties are very similar to those of the mutants for Arg-52 (18,52), suggesting that maintaining the disallowed dihedral angle of Gly-51 is necessary to regulate the direction of the side chain of Arg-52.

Gly-47 of WT has α-helical dihedral angles, and G47A showed pK_a of the chromophore, thermal stability, and photocycle kinetics comparable to WT. However, the absorption maximum of G47A was 3-nm blue shifted. The absorption spectrum of PYP is sensitive to the hydrogen-bonding network composed of the phenolic oxygen of the chromophore, Tyr-42, Glu-46, and Thr-50 (15,18,52). Thus the position of the side chain of Glu-46 is altered in G47A, resulting in the spectral shift.

Gly-37, Gly-59, Gly-86, and Gly-115 have dihedral angles disallowed for alanine (Fig. 1 *b*). They are located at the end of β-strands (Gly-37, Gly-59), the end of an α-helix (Gly-86), or the loop (Gly-115), forming a sharp turn between the secondary structure elements. Replacement of these glycine residues reduced thermal stability, with midtemperatures 4°C–8°C lower than WT. Gly-37 is located between β1 and β2, which are connected by a very compact loop (β-turn). Substitution of alanine into this position is unlikely to allow such a sharp turn, and some hydrogen-bond-forming β-sheet would be broken, resulting in a gain in negative CD signal at 210 nm (Fig. 2 *b*). For G59A, G86A, and G115A, no significant change in the far-UV CD spectrum was observed (Fig. 2 *b*), suggesting that the protein backbone is comparable to that of WT. However, the backbones of these mutants would be constrained at respective positions, resulting in a decrease in thermal stability in the dark state.

In summary, PYP is designed to utilize the flexibility and spatial tolerance of glycine at the right positions. Gly-37, Gly-59, Gly-86, and Gly-115 stabilize the overall structure of PYP. Gly-47 and Gly-51 maintain the chromophore binding site by accommodating key residues (Glu-46 and Arg-52). Gly-77 and Gly-82 regulate the photocycle. The most important glycine location is Gly-29, as it accommodates the carboxylic acid of Glu-46 in its cavity with a CH···O hydrogen bond in the dark-state structure. Once carboxylic acid is negatively charged, hydrophobic packing is broken, and the protein conformational change takes place. These findings are informative for understanding mechanisms of protein folding and structural changes.

This research was financially supported in part by the Global Center of Excellence Program ''Formation of a Strategic Base for Biodiversity and Evolutionary Research: from Genome to Ecosystem'' of the Ministry of Education, Culture, Sports, and Technology (MEXT), Japan.

REFERENCES

1. Baca, M., G. E. Borgstahl, M. Boissinot, P. M. Burke, D. R. Williams, K. A. Slater, and E. D. Getzoff. 1994. Complete chemical structure of photoactive yellow protein: novel thioester-linked 4-hydroxycinnamyl chromophore and photocycle chemistry. *Biochemistry*. 33:14369–14377.
2. Hoff, W. D., P. Düx, K. Hård, B. Devreese, I. M. Nugteren-Roodzant, W. Crielaard, R. Boelens, R. Kaptein, J. van Beeumen, and K. J. Hellingwerf. 1994. Thiol ester-linked *p*-coumaric acid as a new photoactive prosthetic group in a protein with rhodopsin-like photochemistry. *Biochemistry*. 33:13959–13962.
3. Imamoto, Y., T. Ito, M. Kataoka, and F. Tokunaga. 1995. Reconstitution photoactive yellow protein from apoprotein and *p*-coumaric acid derivatives. *FEBS Lett*. 374:157–160.
4. Borgstahl, G. E., D. R. Williams, and E. D. Getzoff. 1995. 1.4 Å structure of photoactive yellow protein, a cytosolic photoreceptor: unusual fold, active site, and chromophore. *Biochemistry*. 34:6278–6287.
5. Getzoff, E. D., K. N. Gutwin, and U. K. Genick. 2003. Anticipatory active-site motions and chromophore distortion prime photoreceptor PYP for light activation. *Nat. Struct. Biol.* 10:663–668.
6. Meyer, T. E. 1985. Isolation and characterization of soluble cytochromes, ferredoxins and other chromophoric proteins from the halophilic phototrophic bacterium *Ectothiorhodospira halophila*. *Biochim. Biophys. Acta*. 806:175–183.
7. Cusanovich, M. A., and T. E. Meyer. 2003. Photoactive yellow protein: a prototypic PAS domain sensory protein and development of a common signaling mechanism. *Biochemistry*. 42:4759–4770.
8. Kort, R., W. D. Hoff, M. Van West, A. R. Kroon, S. M. Hoffer, K. H. Vlieg, W. Crielaand, J. J. Van Beeumen, and K. J. Hellingwerf. 1996. The xanthopsins: a new family of eubacterial blue-light photoreceptors. *EMBO J*. 15:3209–3218.
9. Koh, M., G. Van Driessche, B. Samyn, W. D. Hoff, T. E. Meyer, M. A. Cusanovich, and J. J. Van Beeumen. 1996. Sequence evidence for strong conservation of the photoactive yellow proteins from the halophilic phototrophic bacteria *Chromatium salexigens* and *Rhodospirillum salexigens*. *Biochemistry*. 35:2526–2534.
10. Kort, R., M. K. Phillips-Jones, D. M. van Aalten, A. Haker, S. M. Hoffer, K. J. Hellingwerf, and W. Crielaard. 1998. Sequence, chromophore extraction and 3-D model of the photoactive yellow protein from *Rhodobacter sphaeroides*. *Biochim. Biophys. Acta*. 1385:1–6.
11. Jiang, Z., and E. C. Bauer. 1998. GenBank Accession Number AF064095.
12. Kyndt, J. A., T. E. Meyer, and M. A. Cusanovich. 2004. Photoactive yellow protein, bacteriophytochrome, and sensory rhodopsin in purple phototrophic bacteria. *Photochem. Photobiol. Sci*. 3:519–530.
13. Jiang, Z., L. R. Swem, B. G. Rushing, S. Devanathan, G. Tollin, and C. E. Bauer. 1999. Bacterial photoreceptor with similarity to photoactive yellow protein and plant phytochromes. *Science*. 285:406–409.
14. Van Beeumen, J. J., B. V. Devreese, S. M. Van Bun, W. D. Hoff, K. J. Hellingwerf, T. E. Meyer, D. E. McRee, and M. A. Cusanovich. 1993. Primary structure of a photoactive yellow protein from the phototrophic bacterium *Ectothiorhodospira halophila*, with evidence for the mass and the binding site of the chromophore. *Protein Sci*. 2:1114–1125.
15. Mihara, K., O. Hisatomi, Y. Imamoto, M. Kataoka, and F. Tokunaga. 1997. Functional expression and site-directed mutagenesis of photoactive yellow protein. *J. Biochem. (Tokyo)*. 121:876–880.
16. Kleywegt, G. J., and T. A. Jones. 1996. Phi/psi-chology: Ramachandran revisited. *Structure*. 4:1395–1400.
17. van Aalten, D. M., A. Haker, J. Hendriks, K. J. Hellingwerf, L. Joshua-Tor, and W. Crielaard. 2002. Engineering photocycle dynamics. Crystal

structures and kinetics of three photoactive yellow protein hinge-bending mutants. *J. Biol. Chem.* 277:6463–6468.

18. Imamoto, Y., H. Koshimizu, K. Mihara, O. Hisatomi, T. Mizukami, K. Tsujimoto, M. Kataoka, and F. Tokunaga. 2001. Roles of amino acid residues near the chromophore of photoactive yellow protein. *Biochemistry.* 40:4679–4685.
19. Hirano, S., K. Mihara, Y. Yamazaki, H. Kamikubo, Y. Imamoto, and M. Kataoka. 2002. Role of C-terminal region of *Staphylococcal* nuclease for foldability, stability, and activity. *Proteins Struct. Funct. Genet.* 49:255–265.
20. Imamoto, Y., K. Mihara, F. Tokunaga, and M. Kataoka. 2001. Spectroscopic characterization of the photocycle intermediates of photoactive yellow protein. *Biochemistry.* 40:14336–14343.
21. Ujj, L., S. Devanathan, T. E. Meyer, M. A. Cusanovich, G. Tollin, and G. H. Atkinson. 1998. New photocycle intermediates in the photoactive yellow protein from *Ectothiorhodospira halophila*: picosecond transient absorption spectroscopy. *Biophys. J.* 75:406–412.
22. Harigai, M., Y. Imamoto, H. Kamikubo, Y. Yamazaki, and M. Kataoka. 2003. Role of an N-terminal loop in the secondary structural change of photoactive yellow protein. *Biochemistry.* 42:13893–13900.
23. Ohishi, S., N. Shimizu, K. Mihara, Y. Imamoto, and M. Kataoka. 2001. Light induces destabilization of photoactive yellow protein. *Biochemistry.* 40:2854–2859.
24. Shirai, K., Y. Yamazaki, H. Kamikubo, Y. Imamoto, and M. Kataoka. 2007. Attempt to simplify the amino-acid sequence of photoactive yellow protein with a set of simple rules. *Proteins.* 67:821–833.
25. Meyer, T. E., S. Devanathan, T. Woo, E. D. Getzoff, G. Tollin, and M. A. Cusanovich. 2003. Site-specific mutations provide new insights into the origin of pH effects and alternative spectral forms in the photoactive yellow protein from *Halorhodospira halophila*. *Biochemistry.* 42:3319–3325.
26. Hoff, W. D., B. Devreese, R. Fokkens, I. M. Nugteren-Roodzant, J. Van Beeumen, N. Nibbering, and K. J. Hellingwerf. 1996. Chemical reactivity and spectroscopy of the thiol ester-linked *p*-coumaric acid chromophore in the photoactive yellow protein from *Ectothiorhodospira halophila*. *Biochemistry.* 35:1274–1281.
27. Imamoto, Y., M. Harigai, and M. Kataoka. 2004. Direct observation of the pH-dependent equilibrium between L-like and M intermediates of photoactive yellow protein. *FEBS Lett.* 577:75–80.
28. Meyer, T. E., E. Yakali, M. A. Cusanovich, and G. Tollin. 1987. Properties of a water-soluble, yellow protein isolated from a halophilic phototrophic bacterium that has photochemical activity analogous to sensory rhodopsin. *Biochemistry.* 26:418–423.
29. Shimizu, N., Y. Imamoto, M. Harigai, H. Kamikubo, Y. Yamazaki, and M. Kataoka. 2006. pH-dependent equilibrium between long lived near-UV intermediates of photoactive yellow protein. *J. Biol. Chem.* 281: 4318–4325.
30. Pellequer, J. L., K. A. Wager-Smith, S. A. Kay, and E. D. Getzoff. 1998. Photoactive yellow protein: a structural prototype for the three-dimensional fold of the PAS domain superfamily. *Proc. Natl. Acad. Sci. USA.* 95:5884–5890.
31. Harigai, M., S. Yasuda, Y. Imamoto, K. Yoshihara, F. Tokunaga, and M. Kataoka. 2001. Amino acids in the N-terminal region regulate the photocycle of photoactive yellow protein. *J. Biochem. (Tokyo).* 130: 51–56.
32. van der Horst, M. A., I. H. van Stokkum, W. Crielaard, and K. J. Hellingwerf. 2001. The role of the N-terminal domain of photoactive yellow protein in the transient partial unfolding during signalling state formation. *FEBS Lett.* 497:26–30.
33. Kim, M., R. A. Mathies, W. D. Hoff, and K. J. Hellingwerf. 1995. Resonance Raman evidence that the thioester-linked 4-hydroxycinnamyl chromophore of photoactive yellow protein is deprotonated. *Biochemistry.* 34:12669–12672.
34. Imamoto, Y., K. Mihara, O. Hisatomi, M. Kataoka, F. Tokunaga, N. Bojkova, and K. Yoshihara. 1997. Evidence for proton transfer from Glu-46 to the chromophore during the photocycle of photoactive yellow protein. *J. Biol. Chem.* 272:12905–12908.
35. El-Mashtoly, S. F., M. Unno, M. Kumauchi, N. Hamada, K. Fujiwara, J. Sasaki, Y. Imamoto, M. Kataoka, F. Tokunaga, and S. Yamauchi. 2004. Resonance Raman spectroscopy reveals the origin of an intermediate wavelength form in photoactive yellow protein. *Biochemistry.* 43:2279–2287.
36. Brudler, R., T. E. Meyer, U. K. Genick, S. Devanathan, T. T. Woo, D. P. Millar, K. Gerwert, M. A. Cusanovich, G. Tollin, and E. D. Getzoff. 2000. Coupling of hydrogen bonding to chromophore conformation and function in photoactive yellow protein. *Biochemistry.* 39:13478–13486.
37. Shimizu, N., H. Kamikubo, Y. Yamazaki, Y. Imamoto, and M. Kataoka. 2006. The crystal structure of the R52Q mutant demonstrates a role for R52 in chromophore pK_a regulation in photoactive yellow protein. *Biochemistry.* 45:3542–3547.
38. Anderson, S., S. Crosson, and K. Moffat. 2004. Short hydrogen bonds in photoactive yellow protein. *Acta Crystallogr. D Biol. Crystallogr.* 60:1008–1016.
39. Rajagopal, S., and K. Moffat. 2003. Crystal structure of a photoactive yellow protein from a sensor histidine kinase: conformational variability and signal transduction. *Proc. Natl. Acad. Sci. USA.* 100:1649–1654.
40. Yoda, M., H. Houjou, Y. Inoue, and M. Sakurai. 2001. Spectral tuning of photoactive yellow protein. Theoretical and experimental analysis of medium effects on the absorption spectrum of the chromophore. *J. Phys. Chem. B.* 105:9887–9895.
41. Scheiner, S., T. Kar, and Y. Gu. 2001. Strength of the C^{α} H··O hydrogen bond of amino acid residues. *J. Biol. Chem.* 276:9832–9837.
42. Nishio, M. 2004. Weak hydrogen bonds. *In* Encyclopedia of Supramolecular Chemistry. J. L. Atwood and J. W. Steed, editors. Marcel Dekker, New York. 1576–1585.
43. Nie, B., J. Stutzman, and A. Xie. 2005. A vibrational spectral maker for probing the hydrogen-bonding status of protonated Asp and Glu residues. *Biophys. J.* 88:2833–2847.
44. Brudler, R., R. Rammelsberg, T. T. Woo, E. D. Getzoff, and K. Gerwert. 2001. Structure of the I_1 early intermediate of photoactive yellow protein by FTIR spectroscopy. *Nat. Struct. Biol.* 8:265–270.
45. Xie, A., L. Kelemen, J. Hendriks, B. J. White, K. J. Hellingwerf, and W. D. Hoff. 2001. Formation of a new buried charge drives a large-amplitude protein quake in photoreceptor activation. *Biochemistry.* 40:1510–1517.
46. Derix, N. M., R. W. Wechselberger, M. A. van der Horst, K. J. Hellingwerf, R. Boelens, R. Kaptein, and N. A. van Nuland. 2003. Lack of negative charge in the E46Q mutant of photoactive yellow protein prevents partial unfolding of the blue-shifted intermediate. *Biochemistry.* 42:14501–14506.
47. Pace, C. N., and J. M. Scholtz. 1998. A helix propensity scale based on experimental studies of peptides and proteins. *Biophys. J.* 75:422–427.
48. Rubinstenn, G., G. W. Vuister, F. A. Mulder, P. E. Dux, R. Boelens, K. J. Hellingwerf, and R. Kaptein. 1998. Structural and dynamic changes of photoactive yellow protein during its photocycle in solution. *Nat. Struct. Biol.* 5:568–570.
49. Bernard, C., K. Houben, N. M. Derix, D. Marks, M. A. van der Horst, K. J. Hellingwerf, R. Boelens, R. Kaptein, and N. A. van Nuland. 2005. The solution structure of a transient photoreceptor intermediate: Δ25 photoactive yellow protein. *Structure.* 13:953–962.
50. Joshi, C. P., B. Borucki, H. Otto, T. E. Meyer, M. A. Cusanovich, and M. P. Heyn. 2005. Photoreversal kinetics of the I_1 and I_2 intermediates in the photocycle of photoactive yellow protein by double flash experiments with variable time delay. *Biochemistry.* 44:656–665.
51. Devanathan, S., U. K. Genick, I. L. Canestrelli, T. E. Meyer, M. A. Cusanovich, E. D. Getzoff, and G. Tollin. 1998. New insights into the photocycle of *Ectothiorhodospira halophila* photoactive yellow protein: photorecovery of the long-lived photobleached intermediate in the Met100Ala mutant. *Biochemistry.* 37:11563–11568.
52. Genick, U. K., S. Devanathan, T. E. Meyer, I. L. Canestrelli, E. Williams, M. A. Cusanovich, G. Tollin, and E. D. Getzoff. 1997. Active site mutants implicate key residues for control of color and light cycle kinetics of photoactive yellow protein. *Biochemistry.* 36:8–14.